Journal of Photochemistry and Photobiology A: Chemistry 230 (2012) 31–37

Contents lists available at SciVerse ScienceDirect

Journal of Photochemistry and Photobiology A: Chemistry

journal homepage: www.elsevier.com/locate/jphotochem

Molecular ionization–dissociation of fluoranthene at 266 nm: Energetic and dissociative pathways

J.C. Poveda[a,b,*], I. Álvarez[a], C. Cisneros[a]

[a] Laboratorio de Colisiones Atómicas y Moleculares, Instituto de Ciencias Físicas - UNAM, Cuernavaca, Morelos, Mexico C.P. 62210
[b] Laboratorio de Espectroscopia Atómica Molecular, Escuela de Química - Universidad Industrial de Santander, Bucaramanga, Santander, Colombia A.A. 674

ARTICLE INFO

Article history:
Received 13 March 2011
Received in revised form
13 December 2011
Accepted 30 December 2011
Available online 9 January 2012

Keywords:
Fluoranthene
Polycyclic aromatic hydrocarbons
Photoionization
Dissociation pathways
ToF mass spectrometry

ABSTRACT

Experimental studies have been carried out for nanosecond 266-nm laser-induced photoionization and dissociation of fluoranthene, $C_{16}H_{10}$ with pulse energies from 0.5 to 20 mJ using a time of flight mass spectrometer. The fragmentation patterns have been characterized and discussed with respect to the number of absorbed photons. They fall into three regimes. The first regime involves low energy processes, where the molecular parent ion promptly dissociates, resulting in the formation of $C_mH_n^+ (m = 11 - 15)$ by a process where up to two photons are absorbed. The second regime involves intermediate energy, where dissociative processes are activated by up to three-photon absorption and produce a second group of daughter ions: $C_{10}H_n^+$, $C_9H_n^+$, and $C_8H_n^+$. Finally, there is a third dissociative process, characterized by the absorption of up to four photons, producing $C_7H_n^+$, $C_6H_n^+$, $C_5H_n^+$, $C_4H_n^+$, and $C_3H_n^+$. Most of the detected ions are of the form $C_mH_n^+$ with $m < n$. Total deprotonation has also been observed. The mechanism proposed involves the dissociation of the parent ion, which then dissociates by different competitive channels. Helium, neon and argon were used as carrier gases (CG). A detailed discussion is presented regarding the use of He as the CG. The laser pulse intensity allows the absorption of up to nine photons, observed through the formation of multiply charged ions of some of the CG atoms.

1. Introduction

The polyaromatic hydrocarbon (PAH) fluoranthene is the easiest of the non-alternant PAHs to be synthesized. The spectroscopic characteristics of fluoranthene have been measured and analyzed by several techniques. Its structure offers the interesting possibility of studying unusual behavior: for instance, the topologies of its annular electronic currents offer a phenyl moiety strongly coupled to a naphthalene nucleus as the subject of research.

Fluorescence of jet-cooled fluoranthene had been measured previously [1], and the vibronic progression of the first singlet state has been characterized. The absorption bands of the eight singlet excited states were identified using magnetic circular dichroism, and their transition dipole moments were assigned [2].

Fluoranthene exhibits an anomalous double fluorescence phenomenon, in disagreement with Kasha's rule. This behavior is a consequence of a strong coupling between two electronic states S_1 and S_2, which exhibit a small energy band gap [3,4], as shown in Fig. 1. Usually, the first transition $S_0 \leftarrow S_1$ is known to be weak, while the second transition $S_0 \leftarrow S_2$ is strong. Spectroscopic data reveal other interesting characteristics of the excited state electronic and vibrational structures of fluoranthene [5]. For instance, the vibronic coupling of the S_4 state with the S_3 state has a lifetime greater than 60 fs [6–8].

Other experiments have been carried out: for example, the recombination rates of the cations of ionized fluoranthene were researched, and the infrared spectroscopy of the neutral molecules thus formed and of the cations in the ground state were performed [9–12]. Partial deprotonation of the fluoranthene molecular parent ion was measured using time resolved photoionization in the vacuum UV [13,14], and the total ion photoionization efficiency curve was measured over the photon energy range of 7.5–21.2 eV [14], these works showed that losses of $H^\bullet$ and H_2 are possible, and also that sequential $H^\bullet$ is observed [15]. These phenomena were also observed and discussed by our research group for the naphthalene molecule, as reported in [16]. Multi-photon ionization studies of fluoranthene have been performed in the liquid phase [17–19].

In the present experiments, a cooled fluoranthene molecular beam is photoionized using 266-nm laser radiation. The photophysical characteristics of aromaticity in fluoranthene and the high radiation density ensure that multiphoton ionization occurs. ToF mass spectra as a function of pulse energy in the range of 0.5–20.0 mJ are reported. All ion products are identified. The number of absorbed photons is calculated for each individual ion group

* Corresponding author at: Laboratorio de Colisiones Atómicas y Moleculares, Instituto de Ciencias Físicas - UNAM, Cuernavaca, Morelos, México C.P. 62210. Tel.: +52 777 3172588.
E-mail address: jkclimb@fis.unam.mx (J.C. Poveda).

1010-6030/$ – see front matter © 2012 Elsevier B.V. All rights reserved.
doi:10.1016/j.jphotochem.2011.12.015

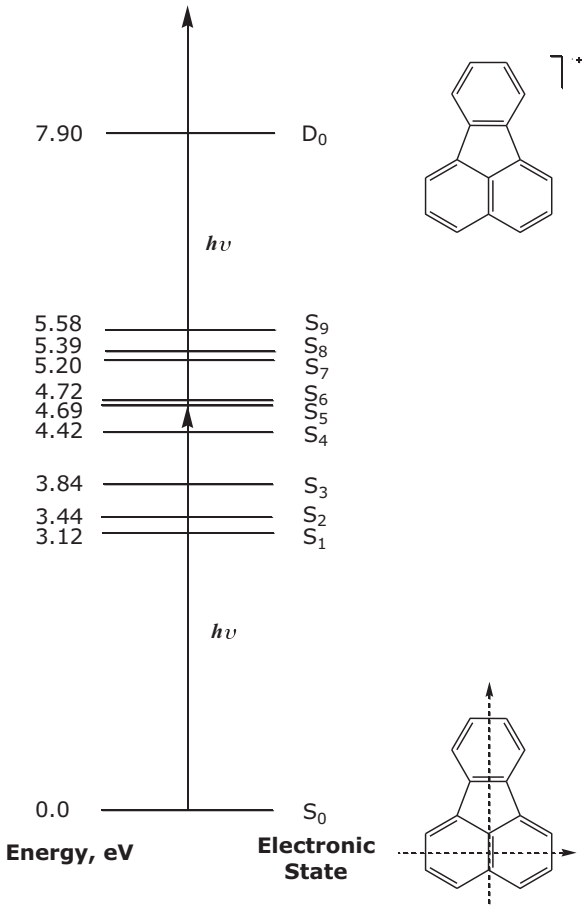

Fig. 1. Electronic states of fluoranthene.

sharing the same number of carbon atoms. Using these results along with the pulse energy at the maximum ion yield, we propose the dissociative channels for the photodestruction of the molecule. Vapors of fluoranthene are introduced into a high-vacuum chamber using He, Ne and Ar as CGs, and their effects are briefly discussed. Although several studies have been carried out on fluoranthene, to the best of our knowledge, multiphoton processes on fluoranthene have not been reported under the conditions presented in this paper.

2. Experimental setup

The photoionization of fluoranthene was analyzed using the experimental setup previously described [20]. A sample of 99.9%-purefluoranthene, purchased from Aldrich Chemical Corp, was used as received. The sample was placed in a thermal chamber and heated up to 373 K to increase its vapor pressure. He, Ne and Ar gases were injected into the thermal chamber at pressures up to 2068 torr and used as CGs to perform independent batches of experiments for comparing the behavior of fluoranthene in each of the three CG's. The mixture of CG and the sample was adiabatically expanded in a high-vacuum chamber at 2×10^{-8} torr, through a pulsed valve synchronized with the laser pulses and with an opening time of 250 μs to reach an operating pressure of 2×10^{-6} torr.

Laser radiation at 266 nm was generated from the fourth harmonic of a Nd:YAG laser at a 30-Hz repetition rate and with a 4.5-ns pulse width. The laser radiation (with a Gaussian profile and linearly polarized) was focused into the interaction region using a lens with a 15-cm focal length. The diameter at the focal point was estimated from the average diameter of the laser spot which was 102.8 μm. Under these experimental conditions, radiation intensities between 10^8 and 10^{10} W cm^{-2} were used.

The cooled molecular beam interacted orthogonally with the laser radiation at a point located between two parallel plates continuously polarized at 5.0 and 4.5 keV, corresponding to the potentials of the extraction and the acceleration plates, respectively. The distance between the plates was 0.8 cm. Holes of 0.5-cm diameter were provided at the center of each plate and were used to extract the positively charged ions. The fragments traversed a field-free region of one-meter length through a pair of electrostatic lenses until they arrived, sequentially in time according to their masses, at the detector located at the end of the ToF analyzer. The signal was pre-amplified, digitalized and sampled in time using a multichannel analyzer EG&G Ortec. Four thousand channels with a 5-ns width time per channel were used, and 5000 laser shots were accumulated and added to obtain the final spectra at the different energies per pulse used in each of the experiments. Several runs were carried out at values between 0.5 and 20 mJ per pulse in order to test the internal consistency of the data.

3. Results and analysis

In the multiphoton regime, molecules can be dissociated by two different mechanisms:

(a) *Ionization–dissociation*: This process is characterized by a fast and efficient multiple photon absorption, which can suppress predissociation channels by a rapid excitation of the electron to the continuum, resulting in the molecule reaching an ionized state. Because the photon absorption can be non-resonant, high photon fluxes are required.
(b) *Dissociation–ionization*: The molecule reaches a vibrational level in an excited state by *n*-photon absorption and dissociates to form daughter fragments, which in turn absorb additional photons to be ionized and/or dissociated once again. If the intermediate excited state has a shorter lifetime than the laser pulse time width, then the neutral fragments absorb additional photons, giving rise to new dissociation or ionization processes.

Fig. 1 shows the electronic states of fluoranthene [21,22] along with the states attainable with the laser energy used in the present experiment. The ToF spectra obtained are plotted in Fig. 2 for different laser intensities while using He as the carrier gas for the fluoranthene.

3.1. Dissociation pathways correlated with the number of absorbed photons

The number of photons absorbed to produce a particular ionization and/or dissociation process can be calculated for a particular ion. The ion current is related to the cross section of the abovementioned processes and to the intensity of radiation by the following expression:

$$Y = f(\sigma_n) I^n \quad (1)$$

where I is the intensity of radiation, and n is the number of absorbed photons, typically equivalent to the smallest number of photons required for a particular species to be ionized. The number of photons is calculated from the experimental data. We have calculated the number of photons required to produce the observed group of ions, $C_mH_n^+$, in the ToF spectra, with m ranging from 1 to 16. The groups were classified based on the number of carbon atoms, from 1 to 16, and the three different carrier gases, as shown in Table 1.

From these results we have identified three different regimes: two, three and four photon absorption, as shown in Fig. 3. To match

Table 1
Effect of carrier gas on the number of absorbed photons.[a]

Ions	Carrier gas		
	Helium	Neon	Argon
$C_2H_n^+$	1.78	1.82	1.44
$C_3H_n^+$	3.68	2.85	2.97
$C_4H_n^+$	3.88	2.84	2.75
$C_5H_n^+$	3.32	2.72	2.43
$C_6H_n^+$	3.21	2.68	2.66
$C_7H_n^+$	3.29	2.91	2.66
$C_8H_n^+$	2.95	3.58	2.70
$C_9H_n^+$	2.47	2.55	2.06
$C_{10}H_n^+$	2.46	2.09	2.00
$C_{11}H_n^+$	2.06	1.77	1.53
$C_{12}H_n^+$	2.09	1.70	1.68
$C_{13}H_n^+$	1.74	1.72	1.16
$C_{14}H_n^+$	1.34	1.33	1.09
$C_{15}H_n^+$	1.57	1.54	1.16
$C_{16}H_n^+$	1.87	1.71	1.47

[a] The analysis takes in account an error of 10% in the calculated number of photons.

the precursors with the daughter ions, the ion currents were normalized to the pulse energy and plotted as a function of the latter. Fig. 4 shows the normalized ion currents for fluoranthene with He used as CG. It can be observed that the maxima of the ion currents are shifted to higher energies as the number of absorbed photons increases. At higher energies per pulse, saturation was reached and new dissociative channels were created by additional photon absorption, which could in turn open additional dissociative channels and produce more daughter ions. The results are summarized in Table 2 for different CGs. The value of the pulse energy at the maximum ion yield is interpreted to be the saturation limit for the particular n photon absorption process, which in turn becomes the threshold of the $n+1$ photon absorption.

3.1.1. Two-photon processes

When the molecule of fluoranthene absorbs one 266-nm photon (4.66 eV), the photon energy is sufficient to excite a high-order vibronic mode of the S_4 electronic state at 4.42 eV, leaving the system with an excess of internal energy. If the second photon is

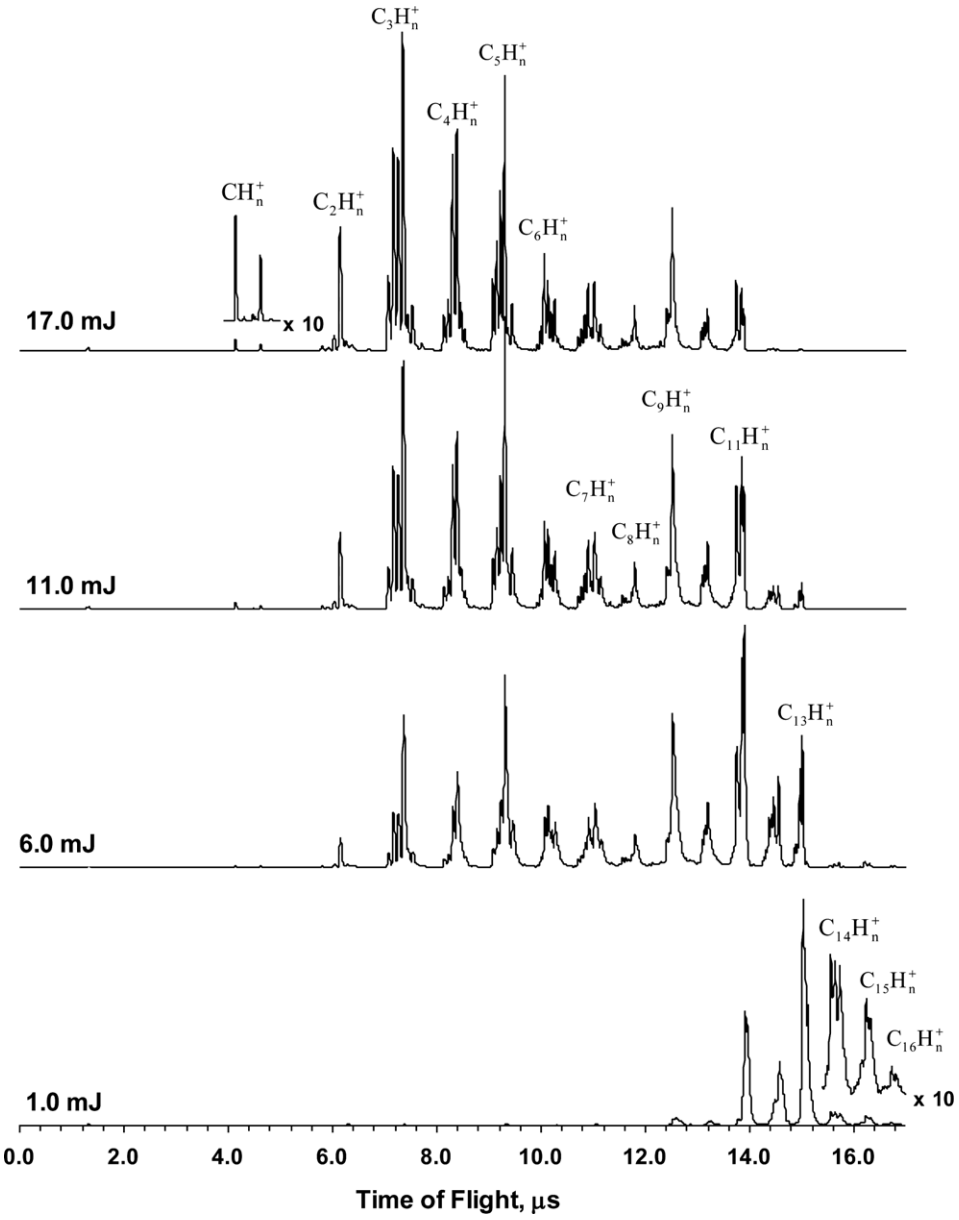

Fig. 2. ToF Spectra of fluoranthene at 266 nm. Helium as carrier gas.

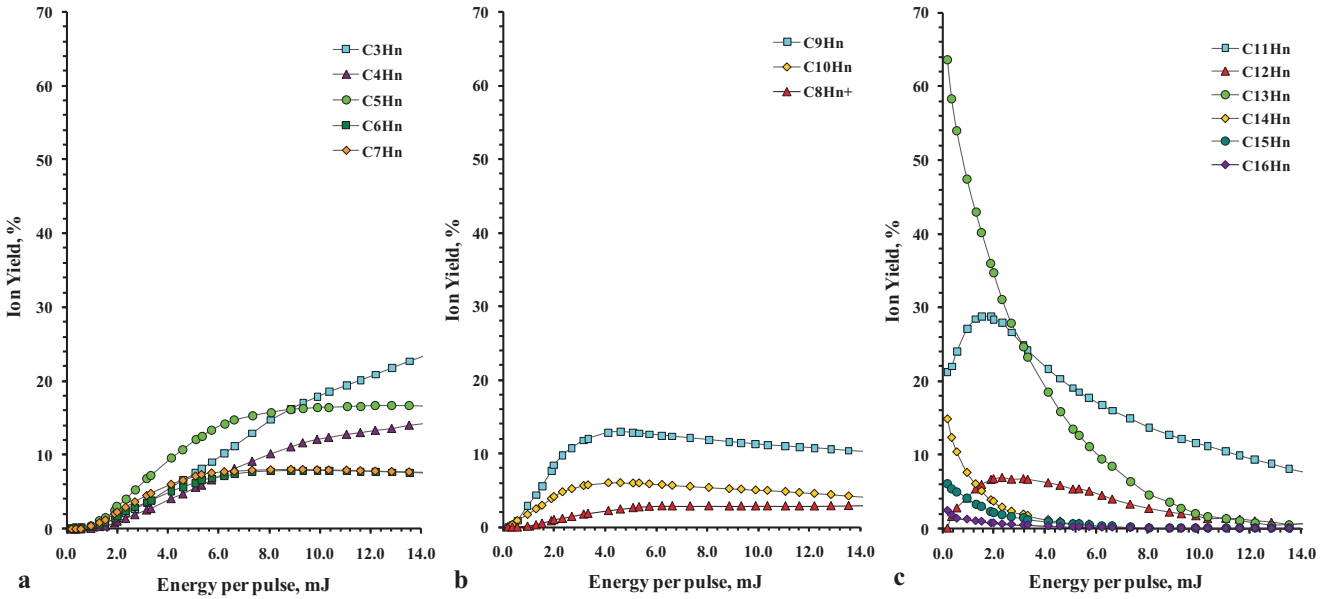

Fig. 3. Relative ion yields. (a) Four-, (b) three-, and (c) two-photon processes. Helium as carrier gas.

absorbed, it allows the molecule to reach an ionized excited state 1.42 eV higher than D_0, as shown in Fig. 1 [21,22]. For low values of pulse energy, the probability that two photons can be absorbed is higher than the probability of the absorption of three or more photons (as shown in Fig. 3), and so on, up to four photons.

Our results show that the molecular parent ion is only observed at very low levels in the interval of energies used here as shown in Fig. 2, disappearing as the pulse energy is progressively increased. It reaches a maximum relative ion current of only 2% at 0.4 mJ per pulse, as shown in Fig. 3. This behavior is the result of fast dissociation processes, which reduce the molecular parent ion population as the probability of three- and four-photon absorption increases and new dissociative channels are opened.

Two-photon absorption allows a molecule to be ionized to a super-excited state, which is followed by a fast dissociation process resulting in a group of daughter ions of the deprotonated species $C_{16}H_n^+$ ($2 \le n \le 10$, n even), along with three groups of daughter ions identified as $C_{15}H_n^+$ ($n < 10$), $C_{14}H_n^+$ ($n < 8$) and $C_{13}H_n^+$ ($6 \le n \le 10$), with the maximum ion yield being produced between pulse energies of 0.85 and 1.08 mJ per pulse, as shown in Table 2, and corresponding to step *i.* in Fig. 5. These values change depending on the CG. The excess energy of the super-excited state enables further dissociation, giving rise to new ion groups: $C_{11}H_n^+$ ($5 \le n \le 10$) and $C_{12}H_n^+$ ($6 \le n \le 10$). Their normalized ion currents show maximum values between 1.61 and 2.13 mJ per pulse. These processes can be represented as follows:

$$C_{16}H_{10}^+ \xrightarrow[-C_2H_q]{-C_3H_q} \begin{matrix} C_{13}H_n^+ \\ C_{14}H_n^+ \\ C_{15}H_n^+ \end{matrix} \xrightarrow{-C_pH_q} \begin{matrix} C_{11}H_n^+ \\ C_{12}H_n^+ \end{matrix} \qquad (2)$$

where $-C_pH_q$ represents a neutral fragment, CH_q or C_2H_q.

The ions $C_2H_n^+$ ($0 \le n \le 5$) were also detected in this energy regime (see Table 1) as a result of two-photon absorption. The maxima of the ion yields were not observed because they were located

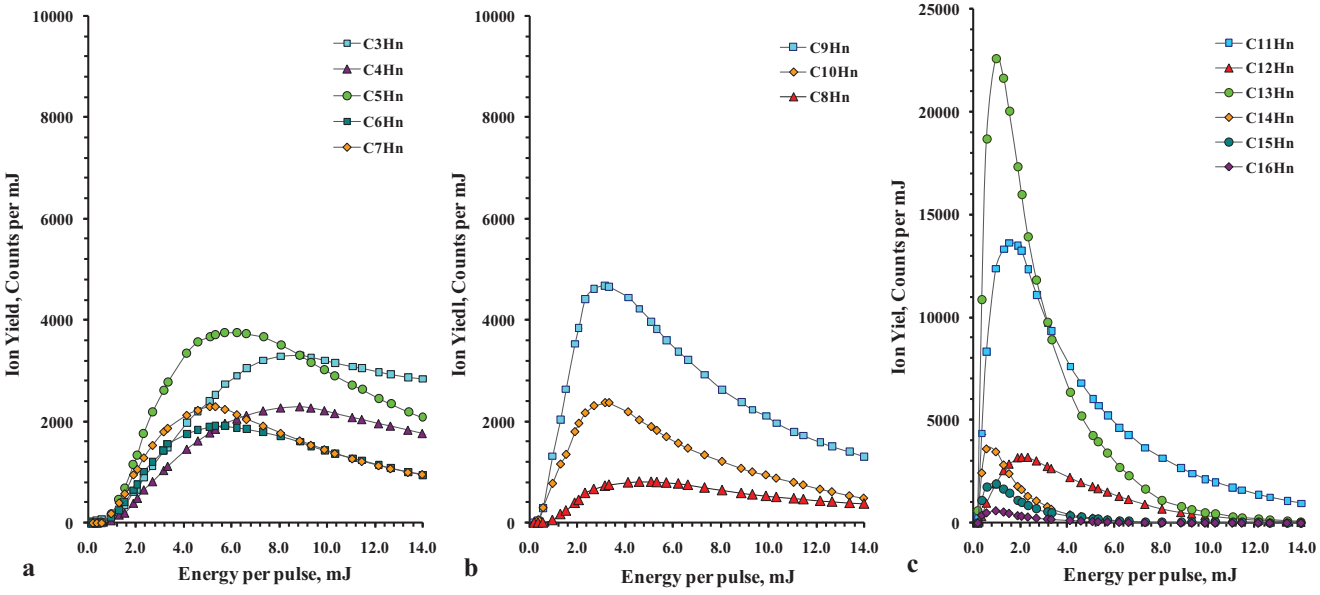

Fig. 4. Normalized ion yields as a function of energy per pulse. (a) Four-, (b) three-, and (c) two-photon processes. Helium as carrier gas.

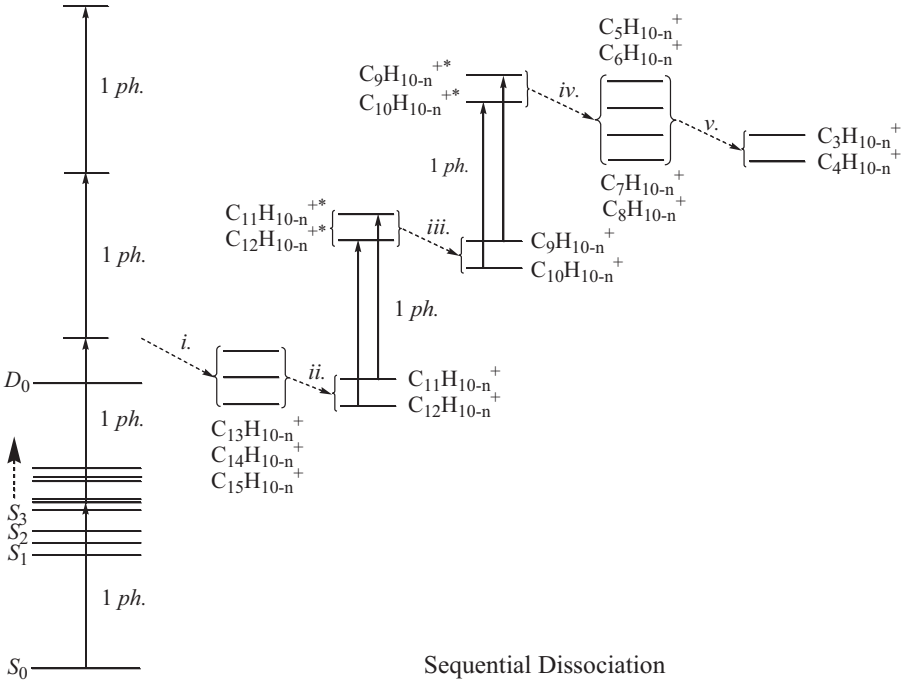

Fig. 5. Dissociation channels as consequence of number of absorbed photons. Helium as carrier gas.

outside the range of the pulse energies of our measurements. The slow increase of the ion yields in response to the increase in the pulse energy suggests that these ions were formed simultaneously with ions originating from other dissociative channels. The loss of neutral acetylene from mono- and di-cations of aromatic molecules constitutes an important dissociative channel. This has been previously discussed in the literature regarding naphthalene ($C_{10}D_8^+ \rightarrow C_8D_6^+ + C_2D_2$, $E_D = 4.41 \pm 0.20$ eV [23,24]), phenanthrene and anthracene ($C_{14}D_{10}^+ \rightarrow C_2D_8^+ + C_2D_2$, $E_D = 4.16$ eV [25]), benzene ($C_6H_6^+ \rightarrow C_4H_4^+ + C_2H_2$, $E_D = 4.16$ eV [26]) and other more complex PAH structures [27–29]. Total photo-destruction of PAHs follows a sequential dissociative mechanism with progressive acetylene loss [15,30]. This mechanism is an adequate explanation for the behavior of the ion current of $C_2H_n^+$ cations observed in the ToF spectra as a function of energy. From our results, we propose that ionized fluoranthene reaches total destruction by sequential acetylene loss as the pulse energy is increased; this is the primary dissociative channel, and accounts for the ion yields of the main ions detected in our ToF spectra in Fig. 6.

3.1.2. Three-photon processes

The three processes can be explained as follows: as the parent molecule dissociates by the absorption of two photons, the daughter ions absorb another photon, resulting in a total energy absorption of 13.98 eV, as shown in Table 1. The maxima in ion yields for each of the daughter ions were reached between 2.4 and 5.8 mJ per pulse and were influenced by the presence of CG, as shown in Table 2. In these cases the saturation limit for the

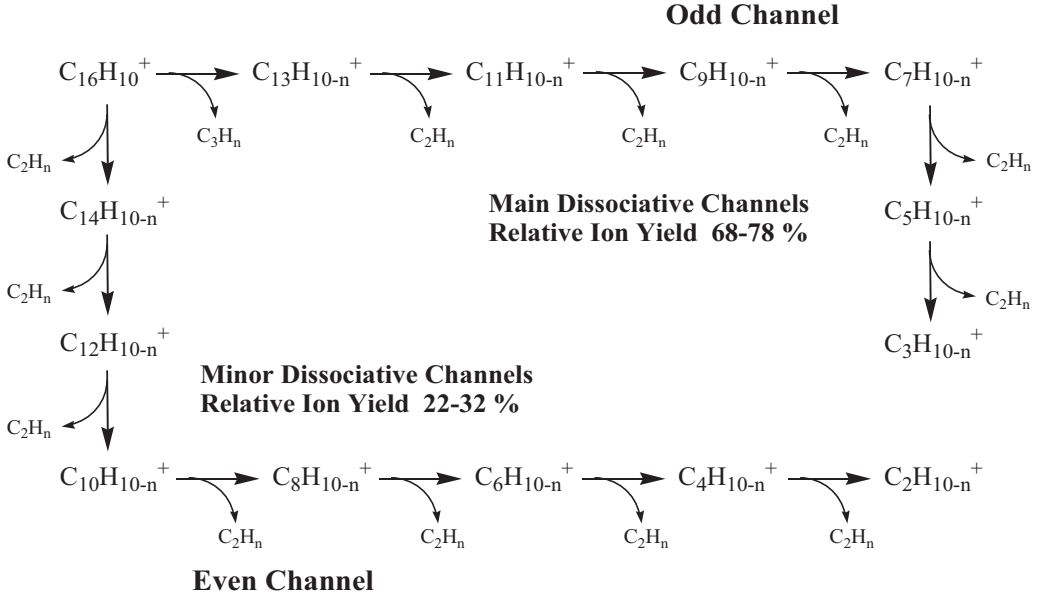

Fig. 6. Main sequential dissociative channels of fluoranthene.

Table 2
Energy per pulse at maximum ion yield.

Ions	Carrier gas		
	Helium	Neon	Argon
$C_2H_n^+$	–	–	–
$C_3H_n^+$	9.09	12.05	10.44
$C_4H_n^+$	8.92	10.70	10.33
$C_5H_n^+$	5.04	9.54	6.80
$C_6H_n^+$	5.10	8.60	6.86
$C_7H_n^+$	4.85	7.57	6.24
$C_8H_n^+$	4.90	7.84	5.79
$C_9H_n^+$	2.69	6.51	3.28
$C_{10}H_n^+$	2.65	4.12	2.43
$C_{11}H_n^+$	1.61	2.62	1.19
$C_{12}H_n$+	2.13	3.57	3.29
$C_{13}H_n^+$	1.08	2.28	1.00
$C_{14}H_n^+$	0.85	1.21	0.93
$C_{15}H_n^+$	0.91	1.32	0.98
$C_{16}H_n^+$	1.02	1.30	1.00

three-photon absorption is the lower limit or the starting point for processes of higher order, e.g., four photons. The dissociative processes that occur via three-photon absorption can be represented as:

$$\begin{matrix} C_{11}H_n^+ \\ C_{12}H_n^+ \end{matrix} \xrightarrow{h\upsilon} \begin{matrix} C_8H_n^+ \\ C_9H_n^+ \\ C_{10}H_n^+ \end{matrix} + C_pH_q \quad (3)$$

Ions resulting from this photon absorption process were identified as $C_8H_n^+$ with n from 1 to 6, $C_9H_n^+$ with n from 3 to 9, and $C_{10}H_n^+$ with n from 6 to 10.

3.1.3. Four-photon processes

Four photons supply an energy equivalent to 18.64 eV, the threshold energy required for the formation of the ions identified as $C_7H_n^+$ with $0 \le n \le 7$, $C_6H_n^+$ with $0 \le n \le 7$, $C_5H_n^+$ with $0 \le n \le 5$, $C_4H_n^+$ with $0 \le n \le 5$, and $C_3H_n^+$ with $0 \le n \le 5$. The dissociation pathways are represented schematically as

$$\begin{matrix} C_8H_n^+ \\ C_9H_n^+ \\ C_{10}H_n^+ \end{matrix} \xrightarrow{h\upsilon} \begin{matrix} C_5H_n^+ \\ C_6H_n^+ \\ C_7H_n^+ \end{matrix} + C_pH_q \xrightarrow{\text{fast diss.}} \begin{matrix} C_3H_n^+ \\ C_4H_n^+ \end{matrix} + C_pH_q \quad (4)$$

Hydrogen transposition processes may take place and contribute to the formation of more ions resulting from four-photon absorption processes: $C_5H_n^+$, $C_6H_n^+$, and $C_7H_n^+$ show maximum ion yield at energies per pulse between 4.85 and 5.10 mJ. At these energies, the dissociation processes reach their maxima and saturation takes place. From our experiment, partial and total deprotonation is observed, evidenced by the detection of C_n^+ ions with n from 1 to 15. At 266 nm, one photon provides the energy for C—H bond breakage, an important process when ions with an odd number of carbon atoms in their structures are generated. If hydrogen was being lost from the ions, it would be eliminated as neutral hydrogen, and not detected in the ToF spectra. On the other hand, if the hydrogen atom loss results in hydrogen cation elimination, it should be detected. Sometimes the detected ions result from non-trivial dissociative processes, and ions with a higher number of hydrogen atoms are observed. For example, CH_n^+ has been detected, with n up to 3. The CH_n^+ formation follows a fourth-order process, and its ion yield increases progressively as the pulse energy increases. These maxima were not observed in the normalized ion currents over all the pulse energy intervals used in our experiments. Therefore, it constitutes an unimportant dissociative channel in the photodestruction of fluoranthene.

3.2. Stability of the molecular parent ion

From our experiments we observed a fast dissociation of the molecular parent ion, which was detected only at low pulse energies (lower than 0.5 mJ) and in quantities lower that 3%, as shown in Fig. 3. The two-photon absorption process supplies an excess of energy (1.42 eV) which is used effectively to open up dissociative channels in the ionized state. This process occurs on a short time scale comparable to that of molecular vibrations. Together with the molecular ionization, high yields for ions with 13 carbon atoms were observed. Ion yields close to 64% at low pulse energies ≅0.25 mJ were obtained. Lower amounts of ion with 14 carbon atoms, approximately 15% at energies per pulse ≅0.25 mJ, were observed in Fig. 3c. The ions with the 13 and the 14 carbon atoms also result from a two-photon absorption process, but with the maxima in ion yield shifted to higher pulse energies. This can be explained by the proposition that the molecular parent ion promptly dissociates three different ways, resulting in $C_{14}H_n^+$, $C_{13}H_n^+$ and $C_{12}H_n^+$, with the simultaneous elimination of neutral fragments with four, three and two carbon atoms, respectively. The results suggest that the elimination of the three-carbon atom neutral fragment is particularly favored over the elimination of the two-carbon atom fragment. These two mechanisms can be represented as:

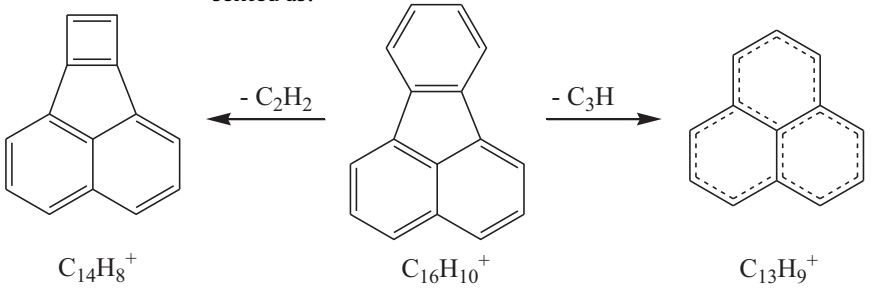

As observed from the ToF spectra and the normalized ion yields in Figs. 2 and 3, the formation of ion groups with an odd number of carbon atoms in their structures is predominant over the formation of those with an even number of carbon atoms. Integrated signals for odd and even ion groups reveal that the relative ion yields reach values between 68–78% for odd ion groups, and 22–32% for even ion groups, as shown in Fig. 6. This behavior suggests that the complete photodestruction of fluoranthene follows two main unique routes, having as their starting point the ions $C_{14}H_n^+$ and $C_{13}H_n^+$ which originated as a consequence of the instability of the molecular parent ion. If acetylene loss is an ingredient of an efficient mechanism for dissociation of heavy ions, energies on the order of one 266-nm photon are required; this has been noted earlier for the case of phenanthrene, benzene, anthracene and naphthalene [23–25]. The complete sequence required to explain the total photodestruction of a fluoranthene molecule by multiple photon absorption and sequential acetylene loss is proposed in Fig. 6. The pathway is energetically favorable and produces ions with an odd number of carbon atoms. By a detailed analysis of the number of absorbed photons and the pulse energy at maximum efficiency for a particular ion, where helium was used as CG, we propose the dissociative

pathways presented in Fig. 5 that lead to the total photodestruction of fluoranthene.

3.3. Effect of carrier gases

In ToF spectra, when CGs were used, the formation of ions of the carrier gas atoms was detected. Isotope patterns led to their unambiguous identification; for instance, $^{20}Ne^{+}$, $^{22}Ne^{+}$ and $^{40}Ar^{+}$ were detected. In addition, multiply charged ions were detected, i.e., $^{20}Ne^{+2}$, $^{22}Ne^{+2}$, $^{40}Ar^{+2}$ and $^{40}Ar^{+3}$ with ionization potentials of 40.96, 27.63 and 40.74 eV, respectively. From these results it is possible to confirm that at the pulse energies used here (0.5–20.0 mJ), the photon densities enable the absorption of up to nine photons.

In Tables 1 and 2, the effect of CGs on the number of absorbed photons and the pulse energies required to reach maximum ion yields for each specific dissociation channel are reported, and compared with the cases where CGs were not used.

The effects of CGs on the number of absorbed photons, their threshold energies for opening new dissociation channels, and their effect on the maxima of ion yields are notorious, as demonstrated by the case of Ne. It has been theoretically demonstrated that the interaction energy of the naphthalene molecule with the CG atom is on the order of some several meV [31,32], and this could be the case for fluoranthene:CG as well. This weak interaction could explain the absence of fluoranthene:CG in the ToF spectra.

4. Conclusions

We have analyzed the photoionization and dissociation of fluoranthene with 266-nm pulses using a ToF apparatus. The experiments were carried out in the multiphoton absorption regime. Three regions of photoionization and photodissociation were analyzed: two-, three- and four-photon absorption. The two photon absorption processes lead to a super-excited electronic state with an excess in energy of 1.42 eV, which allows the molecule to dissociate into two main dissociative channels: $C_{14}H_n^{+}$ and $C_{13}H_n^{+}$. These ions have been identified as the precursors of the two possible main dissociative pathways that result in the total photodestruction of the molecule by a sequential acetylene loss mechanism. Carrier gases He, Ne and Ar were used to allow the sample access to the high vacuum chamber. We propose the full scheme for the total molecular photo-destruction of fluoranthene: the scheme consists of a sequential multistep process of acetylene loss, while using He as the carrier gas. The two main routes produce ions with an odd or even number of carbon atoms in their structure, being in greater abundance the odd ions compared to those with an even number of carbon atoms. The effects of the carrier gases on the number of absorbed photons and on the maxima of the ion yields have also been discussed.

Acknowledgements

This work was financially supported by the DGAPA-UNAM, Grants IN109407 and IN108009, and CONACYT, Grant 24929. The authors thank A. Guerrero for the provision of technical support.

References

[1] I.Y. Chan, M. Dantus, Spectroscopic study of jet-cooled fluoranthene, J. Chem. Phys. 82 (1985) 4471–4476.
[2] J. Kolc, E.W. Thulstrup, J. Michl, Excited singles states of Fluoranthene. I. Absorption linear and magnetic circular dichroism, and polarized fluorescence excitation of the fluorofluoranthenes, J. Am. Chem. Soc. 96 (1974) 7188–7202.
[3] D.L. Philen, R.M. Hedges, S_1 and S_2 fluorescence of fluoranthene, Chem. Phys. Lett. 43 (1976) 358–362.
[4] R.V. Nauman, H.E. Holowan, J.H. Wharton, Comment on S_1 and S_2 fluorescence of fluoranthene, Chem. Phys. Lett. 122 (1985) 523–524.
[5] K.-M. Bark, R.K. Forcé, Observation of dual fluorescence for fluoranthene in the vapor phase, J. Phys. Chem. 93 (1989) 7985–7988.
[6] A.A. Ruth, M.T. Wick, The $S_0 \rightarrow S_4$ transition of jet-cooled Fluoranthene: vibronic coupling of S_4 with S_3, Chem. Phys. Lett. 266 (1997) 206–216.
[7] B. Nickel, Delayed fluorescence from higher excited singlet states of 1 2-benzantracene and fluoranthene, Chem. Phys. Lett. 27 (1974) 84–90.
[8] M. Gehring, B. Nickel, Delayed excimer fluorescence of fluoranthene due to triplet-triplet annihilation: systematic study of the fluorescence from a weakly bound excimer, Z. Phys. Chem. 215 (2001) 343–376.
[9] J. Oomens, G. Meijer, G. Von Helden, Gas phase infrared spectroscopy of cationic indane, acenaphthene, fluorene, and fluoranthene, J. Phys. Chem. A 105 (2001) 8302–8319.
[10] D.M. Hudgins, S.A. Sanford, Infrared spectroscopy of matrix isolated polycyclic aromatic hydrocarbons. 3. Fluoranthene and the benzofluoranthenes, J. Phys. Chem. A102 (1998) 353–360.
[11] P. Klaeboe, Condensed aromatics – XIV. Fluoranthene, Spectrochim. Acta A: Mol. Spectrosc. 37 (1981) 655–661.
[12] C. Rebrion-Rowe, J.L. Le Garrec, M. Hassouna, D. Travers, B.R. Rowe, Experimental evaluation of the recombination rate of cations formed from fluoranthene, Int. J. Mass Spectrom. 223–224 (2003) 237–251.
[13] Ch. Lifshitz, Energetics and dynamics through time-resolved measurements in mass spectrometry: aromatic hydrocarbons, polycyclic aromatic hydrocarbons and fullerenes, Int. Rev. Phys. Chem. 16 (1997) 113–139.
[14] Y. Ling, Ch. Lifshitz, Time-dependent mass spectra and breakdown graphs. 19. Fluoranthene, J. Phys. Chem. 99 (1995) 11074–11080.
[15] F. Jolibois, A. Klotz, F.X. Gadéa, C. Joblin, Hydrogen dissociation of naphthalene cations: a theoretical study, Astron. Astrophys. 444 (2005) 629–634.
[16] J.C. Poveda, A. Guerrero, I. Álvarez, C. Cisneros, Multiphoton ionization and dissociation of Naphthalene at 266, 355, and 532 nm, J. Photochem. Photobiol. A: Chem. 215 (2010) 140–146.
[17] H. Faidas, L.G. Christophorou, Multiphoton ionization of fluoranthene in tetramethylsilane, J. Chem. Phys. 86 (1987) 2505–2509.
[18] G.A. Kourouklins, K. Siomos, L.G. Christophorou, Photoionization of fluoranthene in dielectric liquids, Chem. Phys. Lett. 88 (1982) 572–575.
[19] K. Siomos, L.G. Christophorou, Studies of photoionization in liquids using a laser two-photon ionization conductivity technique, J. Electrostat. 12 (1982) 147–152.
[20] J.C. Poveda, A. San-Román, A. Guerrero, I. Álvarez, C. Cisneros, The effect of the argon carrier gas in the multiphoton dissociation–ionization of tetracene, Int. J. Mol. Sci. 9 (2008) 2003–2015.
[21] O. Birer, P. Moreschini, K.K. Lehmann, Electronic spectroscopy of nonalternat hydrocarbons inside helium nanodrople, J. Phys. Chem. A 111 (2007) 12200–12209.
[22] H. Güsten, G. Heinrich, Photophysical properties of fluoranthene and its benzo analogues, J. Photochem. 18 (1982) 9–17.
[23] M.J. DeWitt, R.J. Levis, Concerning the ionization of large polyatomic molecules with intense ultrafast laser, J. Phys. Chem. 110 (1999) 11368–11375.
[24] S. Leach, J.H.D. Eland, S.D. Price, Formation and dissociation of naphthalene-d_8, J. Phys. Chem. 93 (1989) 7583–7593.
[25] Y. Ling, J.M.L. Martin, Ch. Lifshitz, Energetics of acetylene loss from $C_{14}H_{10}^{+}$ cations: a density functional calculation, J. Phys. Chem. A 101 (1997) 219–226.
[26] H. Kühlewind, A. Kiermeier, H.J. Neusser, Multiphoton ionization in a reflectron time-of-flight mass spectrometer: individual rates of competing dissociation channels in energy-selected benzene cations, J. Chem. Phys. 85 (1996) 4427–4435.
[27] T. Allain, S. Leach, E. Sedlmayr, Photodestruction of PAHs in the interstellar medium I. Photodissociation rates for the loss of an acetylenic group, Astron. Astrophys. 305 (1996) 602–615.
[28] S.J. Pachuta, H.I. Kenttämaa, Th.M. Sack, R.L. Cerny, K.B. Tomer, M.L. Gross, R.P. Pachuta, R.G. Cooks, Excitation and dissociation of isolated ions derived from polycyclic aromatic hydrocarbons, J. Am. Chem. Soc. 110 (1988) 657–665.
[29] W. Cui, B. Hadas, B. Cao, Ch. Lifshitz, Time-resolved photodissociation (TRPD) of the naphthalene and azulene cations in an ion trap/reflectron, J. Phys. Chem. A 104 (2000) 6339–6344.
[30] W.J. van der Hart, Density functional calculations on loss of acetylene from the naphthalene radical cation, Int. J. Mass. Spectrom. 214 (2002) 269–275.
[31] E. Clementi, G. Corongiu, Van der Waals interactions energies of helium, neon, and argon with naphthalene, J. Phys. Chem. A 105 (2001) 10379–10383.
[32] J. Makarewicz, Ab initio potential energy surface and intermolecular vibrations of the naphthalene-argon van der Waals complex, J. Chem. Phys. 134 (2011) 064322-1–064322-8.